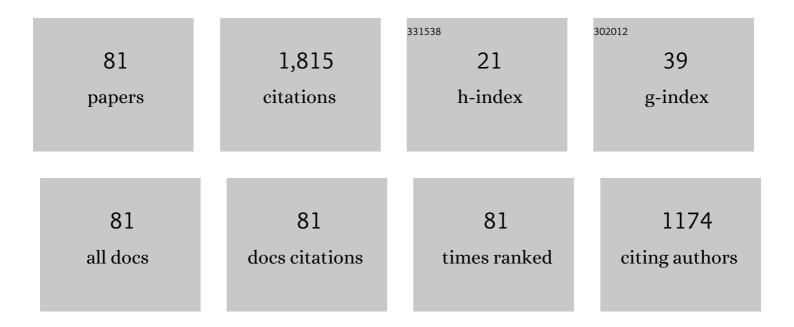
LiangShun Luo

List of Publications by Year in descending order

Source: https://exaly.com/author-pdf/9057718/publications.pdf Version: 2024-02-01



#	Article	IF	CITATIONS
1	Manipulating internal flow units toward favorable plasticity in Zr-based bulk-metallic glasses by hydrogenation. Journal of Materials Science and Technology, 2022, 102, 36-45.	5.6	16
2	Significant enhancement of the corrosion performance of Ti-6Al-3Nb-2Zr-1Mo alloy via carbon addition in reducing acid environment. Materials Letters, 2022, 306, 130939.	1.3	6
3	Effect of processing parameters on the microstructure and mechanical properties of TiAl/Ti2AlNb laminated composites. Journal of Materials Science and Technology, 2022, 109, 228-244.	5.6	19
4	Selective laser melting of high-strength TiB2/AlMgScZr composites: microstructure, tensile deformation behavior, and mechanical properties. Journal of Materials Research and Technology, 2022, 16, 786-800.	2.6	17
5	Effect of growth rate on microstructure evolution in directionally solidified Ti–47Al alloy. Heliyon, 2022, 8, e08704.	1.4	1
6	Corrosion behaviour of a wrought Ti-6Al-3Nb-2Zr-1Mo alloy in artificial seawater with various fluoride concentrations and pH values. Materials and Design, 2022, 214, 110416.	3.3	17
7	Enhanced strength and fracture characteristics of the TiAl/Ti2AlNb laminated composite. Materials Science & Engineering A: Structural Materials: Properties, Microstructure and Processing, 2022, 835, 142632.	2.6	8
8	Microstructure Evolution and Toughening Mechanism of a Nb-18Si-5HfC Eutectic Alloy Created by Selective Laser Melting. Materials, 2022, 15, 1190.	1.3	0
9	In-situ study on Î ³ phase transformation behaviour of Î ³ -TiAl alloys at different cooling rates. Progress in Natural Science: Materials International, 2022, 32, 345-357.	1.8	9
10	Enhanced strength and corrosion resistance in as-cast TA10 alloys via interstitial carbon solute. Materials Research Express, 2022, 9, 046510.	0.8	3
11	Tuning microstructure and improving the corrosion resistance of Ti-6Al-3Nb-2Zr-1Mo alloy using the electron beam freeform fabrication. Chemical Engineering Journal, 2022, 444, 136524.	6.6	9
12	Annealed microstructure dependent corrosion behavior of Ti-6Al-3Nb-2Zr-1Mo alloy. Journal of Materials Science and Technology, 2021, 62, 234-248.	5.6	68
13	In-situ investigation of β/α transformation in β-solidifying γ-TiAl alloys at different cooling rates. Materials Letters, 2021, 285, 129092.	1.3	6
14	The corrosion behavior of Ti-6Al-3Nb-2Zr-1Mo alloy: Effects of HCl concentration and temperature. Journal of Materials Science and Technology, 2021, 74, 143-154.	5.6	43
15	The interface structure and its impact on the mechanical behavior of TiAl/Ti2AlNb laminated composites. Materials Science & Engineering A: Structural Materials: Properties, Microstructure and Processing, 2021, 827, 142095.	2.6	14
16	Design a novel TiAl/Ti2AlNb laminated composite with high toughness prepared by foil-foil metallurgy. Materials Letters, 2021, 303, 130463.	1.3	8
17	Effect of zirconium content on the microstructure and corrosion behavior of as-cast Ti-Al-Nb-Zr-Mo alloy. Journal of Materials Research and Technology, 2021, 15, 4896-4913.	2.6	31
18	Microstructures and mechanical properties of Ti–44Al–5Nb–3Cr–1.5Zr–xMo–yB alloys. Journal of Materials Research, 2020, 35, 2756-2764.	1.2	4

#	Article	IF	CITATIONS
19	Thermal deformation behavior of \hat{I}^3 -TiAl based alloy by plasma hydrogenation. International Journal of Hydrogen Energy, 2020, 45, 34214-34226.	3.8	6
20	Effect of melt hydrogenation on microstructure evolution and tensile properties of (TiB +â€TiC)/Ti-6Al-4V composites. Journal of Materials Research and Technology, 2020, 9, 6343-6351.	2.6	10
21	Microstructural Optimization of Feâ€Rich Intermetallic in Al–12 wt% Si–2 wt% Fe alloys by Adding Travelling Magnetic Fields. Advanced Engineering Materials, 2020, 22, 2000561.	1.6	0
22	Impact of hydrogen microalloying on the mechanical behavior of Zr-bearing metallic glasses: A molecular dynamics study. Journal of Materials Science and Technology, 2020, 45, 198-206.	5.6	16
23	Investigation of shear transformation zone and ductility of Zr-based bulk metallic glass after plasma-assisted hydrogenation. Materials Science & Engineering A: Structural Materials: Properties, Microstructure and Processing, 2019, 759, 105-111.	2.6	21
24	Hot-deformation behaviour and hot-processing map of melt-hydrogenated Ti 6Al 4V/(TiB+TiC). International Journal of Hydrogen Energy, 2019, 44, 8641-8649.	3.8	18
25	Microstructure and Mechanical Properties of Bioâ€Inspired Ti/Al/Al _f Multilayered Composites. Advanced Engineering Materials, 2019, 21, 1800722.	1.6	2
26	Effects of hydrogen on the interfacial reaction between Ti 6Al 4V alloy melt and Al2O3 ceramic shell. International Journal of Hydrogen Energy, 2018, 43, 5225-5230.	3.8	3
27	Hydrogen induced microstructure evolution of titanium matrix composites. International Journal of Hydrogen Energy, 2018, 43, 9838-9847.	3.8	16
28	New insights into melt hydrogenation effects on glass-forming ability in a Zr-based bulk metallic glass. Journal of Non-Crystalline Solids, 2018, 481, 170-175.	1.5	4
29	Positive effect of hydrogen on interface of in situ synthesized Ti-6Al-4V matrix composites. Materials Science & Engineering A: Structural Materials: Properties, Microstructure and Processing, 2018, 711, 12-21.	2.6	8
30	Nanometer-scale gradient atomic packing structure surrounding soft spots in metallic glasses. Npj Computational Materials, 2018, 4, .	3.5	37
31	Hydrogen induced softening and hardening for hot workability of (TiBÂ+ÂTiC)/Ti-6Al-4V composites. International Journal of Hydrogen Energy, 2017, 42, 3380-3388.	3.8	16
32	Effect of gallium addition on the microstructure and micromechanical properties of constituents in Nb Si based alloys. Journal of Alloys and Compounds, 2017, 704, 89-100.	2.8	40
33	High temperature deformation behavior of melt hydrogenated (TiB + TiC)/Ti-6Al-4V composites. Materials and Design, 2017, 121, 335-344.	3.3	33
34	Effects of hydrogen on the nanomechanical properties of a bulk metallic glass during nanoindentation. International Journal of Hydrogen Energy, 2017, 42, 25436-25445.	3.8	14
35	Microstructures and mechanical properties of melt hydrogenated Nb-Si based alloy. International Journal of Hydrogen Energy, 2017, 42, 26417-26422.	3.8	4
36	Hot deformation behavior and dynamic recrystallization of melt hydrogenated Ti-6Al-4V alloy. Journal of Alloys and Compounds, 2017, 728, 709-718.	2.8	32

#	Article	IF	CITATIONS
37	Hydrogen-induced amorphization of Zr-Cu-Ni-Al alloy. China Foundry, 2017, 14, 145-150.	0.5	Ο
38	Effect of hydrogen addition on the mechanical properties of a bulk metallic glass. Journal of Alloys and Compounds, 2017, 695, 3183-3190.	2.8	19
39	Mechanical properties of microconstituents in Nb-Si-Ti alloy by micropillar compression and nanoindentation. Materials Science & Engineering A: Structural Materials: Properties, Microstructure and Processing, 2017, 687, 99-106.	2.6	24
40	Microstructures, micro-segregation and solidification path of directionally solidified Ti-45Al-5Nb alloy. China Foundry, 2016, 13, 107-113.	0.5	11
41	Effect of growth rate on microstructures and microhardness in directionally solidified Ti–47Al–1.0W–0.5Si alloy. Journal of Materials Research, 2016, 31, 618-626.	1.2	3
42	Comparison of microstructures and mechanical properties of as-cast and directionally solidified Ti-47Al-1W-0.5Si alloy. Journal of Alloys and Compounds, 2016, 682, 663-671.	2.8	32
43	Lamellar orientation control of Ti–47Al–0.5W–0.5Si by directional solidification using β seeding technique. Intermetallics, 2016, 73, 1-4.	1.8	8
44	Microstructure and mechanical properties of in-situ MC-carbide particulates-reinforced refractory high-entropy Mo0.5NbHf0.5ZrTi matrix alloy composite. Intermetallics, 2016, 69, 74-77.	1.8	72
45	Influence of thermal stabilization treatment on microstructure evolution of the mushy zone and subsequent directional solidification in Ti-43Al-3Si alloy. Materials and Design, 2016, 97, 392-399.	3.3	14
46	Microstructure and mechanical properties of refractory high entropy (Mo 0.5 NbHf 0.5 ZrTi) BCC /M 5 Si 3 in-situ compound. Journal of Alloys and Compounds, 2016, 660, 197-203.	2.8	83
47	Hot deformation characteristics and dynamic recrystallization of the MoNbHfZrTi refractory high-entropy alloy. Materials Science & Engineering A: Structural Materials: Properties, Microstructure and Processing, 2016, 651, 698-707.	2.6	107
48	Effect of composing element on microstructure and mechanical properties in Mo–Nb–Hf–Zr–Ti multi-principle component alloys. Intermetallics, 2016, 69, 13-20.	1.8	55
49	A Mathematical Model for Determination of Lamellar Spacing in Materials of Poly-Grain Microstructures. Rare Metal Materials and Engineering, 2015, 44, 272-276.	0.8	Ο
50	Sampling period online adjusting-based hysteresis current control without band with constant switching frequency. IEEE Transactions on Industrial Electronics, 2015, 62, 270-277.	5.2	61
51	Microstructure and mechanical properties of refractory MoNbHfZrTi high-entropy alloy. Materials & Design, 2015, 81, 87-94.	5.1	261
52	Effects of Input Harmonics, DC Offset and Step Changes of the Fundamental Component on Single-Phase EPLL and Elimination. Journal of Power Electronics, 2015, 15, 1085-1092.	0.9	2
53	Microstructure and mechanical properties of ZrNbMoHfV high entropy alloy. Materials Research Innovations, 2014, 18, S4-766-S4-769.	1.0	4
54	The influence of melt hydrogenation on Ti600 alloy. International Journal of Hydrogen Energy, 2014, 39, 6089-6094.	3.8	9

#	Article	IF	CITATIONS
55	Stability of remelting and solidification interfaces of triple-phase region during peritectic reaction at lower speed. Transactions of Nonferrous Metals Society of China, 2014, 24, 1951-1958.	1.7	1
56	Influence of initial solid–liquid interface morphology on further microstructure evolution during directional solidification. Applied Physics A: Materials Science and Processing, 2013, 110, 443-451.	1.1	6
57	A lateral remelting phenomenon of the primary phase below the temperature of peritectic reaction in directionally solidified Cu–Ge alloys. Journal of Materials Research, 2013, 28, 3261-3269.	1.2	11
58	Two-phase separated growth and peritectic reaction during directional solidification of Cu–Ge peritectic alloys. Journal of Materials Research, 2013, 28, 1372-1377.	1.2	5
59	Characterization of hydrogen-induced structural changes in Zr-based bulk metallic glasses using positron annihilation spectroscopy. Journal of Materials Research, 2012, 27, 2587-2592.	1.2	4
60	Fabrication of wavy γ-TiAl based sheet with foil metallurgy. Transactions of Nonferrous Metals Society of China, 2012, 22, 72-77.	1.7	7
61	Isothermal Peritectic Coupled Growth in Directionally Solidified Cu-20ÂwtÂpct Sn Alloy. Metallurgical and Materials Transactions A: Physical Metallurgy and Materials Science, 2012, 43, 4219-4223.	1.1	4
62	Solute redistribution during planar growth of intermetallic compound with nil solubility. Intermetallics, 2012, 26, 131-135.	1.8	21
63	Morphological characteristics of triple junction region and process of the peritectic reaction during directional solidification of Cu–Ge alloys. Journal of Alloys and Compounds, 2012, 539, 44-49.	2.8	8
64	Influences of Fe and B on the Columnar Structure of Ti-46Al Alloys. Rare Metal Materials and Engineering, 2012, 41, 570-574.	0.8	8
65	Enhanced plasticity in Zr-based bulk metallic glasses by hydrogen. International Journal of Hydrogen Energy, 2012, 37, 14697-14701.	3.8	42
66	Gradient microstructure of TC21 alloy induced by hydrogen during hydrogenation. International Journal of Hydrogen Energy, 2012, 37, 19210-19218.	3.8	20
67	Bulk metallic glass formation: The positive effect of hydrogen. Journal of Non-Crystalline Solids, 2012, 358, 2606-2611.	1.5	17
68	Study on in situ Al-Si functionally graded materials produced by traveling magnetic field. Science and Engineering of Composite Materials, 2012, 19, 209-214.	0.6	4
69	Secondary dendrite arm migration caused by temperature gradient zone melting during peritectic solidification. Acta Materialia, 2012, 60, 2679-2688.	3.8	41
70	Deoxidation of bulk metallic glasses by hydrogen arc melting. Materials Letters, 2012, 83, 1-3.	1.3	12
71	First Phase Selection in Solid Ti/Al Diffusion Couple. Rare Metal Materials and Engineering, 2011, 40, 753-756.	0.8	21
72	An analysis of non-equilibrium peritectic reaction driven by solute diffusion under a temperature gradient. Journal of Crystal Growth, 2011, 334, 195-199.	0.7	10

#	Article	IF	CITATIONS
73	Directional Solidification of TiAl-Based Alloys: Determination of the Primary Phase in Ti-50Al-5Nb Alloy. Rare Metal Materials and Engineering, 2011, 40, 1-3.	0.8	6
74	Investigation of melt hydrogenation on the microstructure and deformation behavior of Ti–6Al–4V alloy. International Journal of Hydrogen Energy, 2011, 36, 1027-1036.	3.8	29
75	Hydrogen solubility in molten TiAl alloys. International Journal of Hydrogen Energy, 2010, 35, 8008-8013.	3.8	23
76	Deoxidation of Ti–Al intermetallics via hydrogen treatment. International Journal of Hydrogen Energy, 2010, 35, 9214-9217.	3.8	17
77	Effect of hydrogen on hot deformation behaviors of TiAl alloys. International Journal of Hydrogen Energy, 2010, 35, 13322-13328.	3.8	35
78	Deoxidation of Titanium alloy using hydrogen. International Journal of Hydrogen Energy, 2009, 34, 8958-8963.	3.8	53
79	A simple model for lamellar peritectic coupled growth with peritectic reaction. Science in China Series C: Physics, Mechanics and Astronomy, 2007, 50, 442-450.	0.2	4
80	Formation of titanium hydride in Ti–6Al–4V alloy. Journal of Alloys and Compounds, 2006, 425, 140-144.	2.8	63
81	Well-aligned in situ composites in directionally solidified Fe–Ni peritectic system. Applied Physics Letters, 2006, 89, 231918.	1.5	19